# Physiological Basis of Limb-Impedance Modulation During Free and Constrained Movements

**Loïc Damm and Joseph McIntyre**

**You might find this additional info useful...**

This article cites 40 articles, 17 of which can be accessed free at:
http://jn.physiology.org/content/100/5/2577.full.html#ref-list-1

This article has been cited by 1 other HighWire hosted articles

**Impedance Control Reduces Instability That Arises from Motor Noise**
Luc P. J. Selen, David W. Franklin and Daniel M. Wolpert
*J. Neurosci.*, October, 7 2009; 29 (40): 12606-12616.
[Abstract] [Full Text] [PDF]

Updated information and services including high resolution figures, can be found at:
http://jn.physiology.org/content/100/5/2577.full.html

Additional material and information about *Journal of Neurophysiology* can be found at:
http://www.the-aps.org/publications/jn

This infomation is current as of February 14, 2011.

# Physiological Basis of Limb-Impedance Modulation During Free and Constrained Movements

**Loïc Damm and Joseph McIntyre**

*Laboratoire de Physiologie de la Perception et de l'Action, Centre National de la Recherche Scientifique, Collège de France; and Laboratoire de Neurobiologie des Réseaux Sensorimoteurs, CNRS UMR 7060, Université Paris Descartes, 75006 Paris, France*

**Damm L, McIntyre J.** Physiological basis of limb-impedance modulation during free and constrained movements. *J Neurophysiol* 100: 2577–2588, 2008. First published August 20, 2008; doi:10.1152/jn.90471.2008. Arm stiffness is a critical factor underlying stable interactions with the environment. When the hand moves freely through space, a stiff limb would most effectively maintain the hand on the desired path in the face of external perturbations. Conversely, when constrained by a rigid surface, a compliant limb would allow the surface to guide the hand while minimizing variations in contact forces. We aimed to identify the physiological basis of stiffness adaptation for these two classes of movement. Stiffness can be regulated by two mechanisms: coactivation of antagonistic muscles and modulation of reflex gains. We hypothesized that subjects would select high stiffness (high coactivation and/or reflex gains) in free space and high compliance (low coactivation and reflex gains) for constrained movements. We measured EMG and the H-reflex during constrained and unconstrained movement of the wrist. As predicted, subjects coactivated antagonist muscles more when performing the unconstrained movement. Contrary to our hypothesis, however, H-reflex amplitude was higher for the constrained movement despite the a priori preference for lower reflex gains in this situation. In addition, the H-reflex depended on the task and the net force exerted by the limb on the environment, rather than showing a simple dependence on the level of muscle activation. Thus stiffness seems to increase in free space compared with constrained motion through the use of coactivation, whereas spinal loop gains are adjusted to better regulate the influence of afferences on the ongoing movement. These observations support the hypothesis of movement programming in terms of impedance.

## INTRODUCTION

When performing tasks with the arm and hand, the sensorimotor system must not only program the motion of the limb and the forces to exert against the environment; or attention to how unexpected forces and displacements should be handled is also of primary importance. Different tasks may require distinct types of control in this respect. For example, if the path of the hand is constrained by solid objects in certain dimensions, the edges of the object can guide the movement. In this way, one might make use of a rigid wall to find a light switch in the absence of any visual information.

When the hand slides along a wall, if the geometry of the wall does not match the trajectory anticipated by the motor command, the motor system will most efficiently manage the task by complying with the constraints imposed by the rigid surface. On the other hand, when the hand moves freely through space, a compliant limb would be ineffective at following the appropriate path in the case of an external perturbation or unexpected force. Control of limb stiffness or, more generally, control of limb *impedance*, would appear to reconcile the requirements of both types of tasks. A high stiffness or a high compliance would be selected according to the task to be performed. Task-dependent changes of mechanical impedance of the limb have been reported that depend on a number of different factors, including instruction (Evarts and Tanji 1974; Hammond 1956), the direction of succeeding movements (Tanji and Evarts 1976), the resistance applied to perturbations (Lacquaniti et al. 1982), and movement accuracy (Selen et al. 2006). By coupling an unstable load to a finger, Akazawa and colleagues (1983) noted the propensity of the CNS to coactivate antagonistic muscles. The CNS is able to regulate the shape and the orientation of the stiffness matrix in an unstable environment (Burdet et al. 2001; Franklin et al. 2003; Milner 2002). Moreover, the magnitude of stiffness increase depends on the degree of instability (Franklin et al. 2004). Here we ask a related question: How does the CNS regulate stiffness based on the relative stability of the interaction with the environment?

How can the CNS modulate impedance? First, the agonist–antagonist architecture of the muscular system allows for impedance control by the CNS (Hogan 1984; Houk and Rymer 1981; Humphrey and Reed 1983; Smith 1981). Because the stiffness of the muscle is dependent on its activation, the CNS can affect the mechanical impedance of the limb by adjusting alpha-motoneuron activation in opposing muscles.[1] Another mechanism potentially used by the CNS to regulate limb impedance is reflex (Nichols and Houk 1976). The reflex activation of the muscles can also resemble that of a spring in that stretching the muscles induces increased activation and force. Consequently, this active system can mimic the behavior of a passive endpoint impedance (Hogan 1990), the stiffness of which depends on the influence of upper centers on spinal loop gains. Thus there are two principal mechanisms by which the CNS can regulate limb stiffness: coactivation and reflex gain modulation.

For the upper limb, the factors that determine the levels of coactivation and reflex gains during skilled movements remain

---

[1] In this respect, we should distinguish between alpha-motoneuron activation that has an influence on the forward path so as to generate net force and mechanisms such as coactivation or spinal reflexes, which can affect the intrinsic impedance of the system.

to be identified, yet these two mechanisms for impedance control can be studied experimentally in humans. Measurements of surface electromyogram (EMG) provide a means of evaluating coactivation during movement, whereas the measure of the H-reflex can be used to infer the contribution of peripheral afferences to motoneuron activity during movements. In the experiment reported here, we examined two classes of movement, constrained or free. Subjects were instructed to slide the hand along a rigid surface or to follow a prescribed path in free space while we measured EMG and the H-reflex. We hypothesized that mechanisms aiming to increase impedance should be enhanced in free versus constrained movements. As we will show, this hypothesis was only partially borne out.

## METHODS

### Participants

The investigation was carried out on eight volunteer subjects, aged 25–33 yr, who were right-handed and had no known problems of motor control. They gave their informed consent to the experimental procedure, which was approved by the local ethics committee and carried out in compliance with French law and the Helsinki declaration.

### Force actuated joystick and virtual reality setup

The experiments were carried out in the virtual haptic setup shown in Fig. 1, as used previously (McIntyre et al. 1995). The experimental setup was equipped with a seat, a force-actuated joystick, and a video screen connected to a computer to display the virtual scene and to give instructions to the subject (procedure to be used, test number, etc.). The two-dimensional, force-actuated joystick (ROBOTOP, Matra-Marconi Space) was attached to the right side of the chair, positioned in line with the shoulder at a distance of 0.5 m in front of the subject. It was oriented such that its axis projected horizontally toward the



FIG. 1. Subject seated in the experimental setup. The virtual scene was presented on the screen in front of the subject. To manipulate the ROBOTOP joystick with the right hand, subjects rested their forearm in a plastic trough that restricted all movements of the arm except those at the wrist.

subject when the joystick was at its center position. Movements of the joystick were in a plane parallel to that of the video monitor, with the $x$-axis and $y$-axis corresponding to horizontal and vertical movements, respectively.

To keep the elbow angle constant and prevent any movement at the shoulder, subjects rested their forearm in a plastic trough that restricted all movements of the arm except those at the wrist. With the right hand on the joystick grip and the joystick centered in its range of motion, both the joystick shaft and the forearm of the subject were oriented horizontally. The forearm was pronated. Subjects held a spherical handgrip attached to a 150-mm shaft whose bearing mechanism allowed rotational movements about two perpendicular axes. The grip was thus free to move along the surface of a sphere that we considered to be a planar surface. On each axis, the shaft rotated $\pm 25°$ from the center position, providing $\pm 6.3$ cm of linear range with a maximum deviation of 2.2 cm from the plane. The motors provided a maximum feedback force of 25 N. An optical encoder measured shaft position with a resolution of 0.09 mm at the endpoint. The grip was equipped with a two-axis force sensor having a range of $\pm 40$ N and a resolution of 0.02 N. This system was able to simulate different types of constraints such as a constant force field or contact with a rigid surface (for a description of the joystick performance, see McIntyre et al. 1995).

### Virtual environment and experimental tasks

Subjects were required to displace a small rectangular object, a peg, which moved on the screen according to the position of the joystick. Movements of the joystick evoked parallel movements of the peg on the screen. We defined two physical environments based on the interaction subjects had to manage during the movement: free or constrained. Both environments included a free rectangular area, without constraint, delimited by four walls (Fig. 2).

### Constrained environment: surface following (SF)

For the constrained motion task, subjects were required to slide the hand along the lower surface of the virtual environment. This virtual surface included a small hole on the right part of the lower wall, which constituted the goal for the sliding movement. At the beginning of every trial, the peg appeared on the top left corner of the workspace. Subjects had to lower the peg toward the virtual surface and then slide the peg along the horizontal surface until it reached the hole. The trial was then automatically ended.

### Free environment: path following (PF$_0$)

The free environment differed from that used in the preceding constrained case in that the bottom surface was lower and had no hole. Instead, a green line extended horizontally in the free area of the workspace above the lower surface, at the same vertical location as the lower surface used in the SF condition. Unlike the solid walls limiting the workspace, the green line was not a physical obstacle but a purely visual guide for the movement. The initial position of the peg was the same as that in the constrained environment, i.e., in the top left corner. Subjects were required to lower the peg until they aligned its center with the green line and then follow this path. Once they reached the right extremity of the line, they were instructed to lower the peg below the line to finish the trial. The path described by the colored line was therefore equivalent to the path followed when sliding the peg along the surface toward the hole.

Subjects were trained during 30 trials to follow the correct path by ensuring that the peg overlapped the green line. The line represented approximately one tenth of the visual height of the peg. Maintaining the peg on the line allowed a margin of error in the vertical hand placement of $\pm 0.6$ cm. Subjects easily obtained this level of performance after a few trials. No penalty was given to the subject during
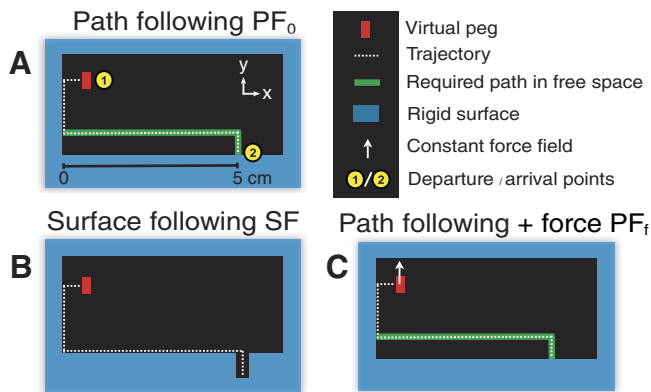
## Path following PF$_0$



FIG. 2. Virtual scene viewed by subjects. Blue edges represented rigid surfaces. For each condition, the task was to displace the peg along the trajectory symbolized by the dashed line (not visible in the virtual scene). Measures were collected while subjects completed the horizontal portion of the trajectory. A: path following condition (PF$_0$). Subjects followed the horizontal path in free space. The green line is a purely visual landmark. B: surface following condition (SF). Subjects slid along the horizontal surface and were instructed to maintain the contact against it. C: path following + force condition (PF$_f$). Similar to PF$_0$, but in addition subjects had to counteract the effects of a constant upward force applied by the joystick.

the test trials for failing to remain on the line, but during the analysis, trials with trajectories that did not remain on the reference line were discarded. Such trials were rare and were easily distinguished from the average.

### Free environment: path following with bias force (PF$_f$)

The two types of movements described earlier differed primarily in terms of the type of constraint imposed on the path of the hand—physical in the case of hand-sliding versus visual in the case of free movement. However, the movements also differed in terms of the net force exerted by the arm in the vertical direction, perpendicular to the path of the movement. In the surface-following task, the hand exerted a contact force against the physical constraint, whereas in the path-following movement the net force at the hand was close to zero. This difference in the exerted force could conceivably complicate the interpretation of the H-reflex data, since it is known that H-reflex amplitude depends on the background level of muscle activation (Matthews 1986a). To control for this difference, we devised a third condition in which there was no rigid constraint. Instead, the subject followed the trajectory indicated by the green line, as in the condition PF$_0$. At the same time, however, the joystick applied a constant, upward bias force to the hand. The magnitude of this force was the same everywhere in the workspace and was chosen to be at least equal to the force subjects exerted on the virtual surface in the SF condition (based on pilot trials). Thus to remain on the line the subject had to exert a downward force to counteract the bias force from the joystick. This force bias could not, however, guide the movement because the peg was free to move below the level of the green line. The subject was responsible for controlling the path followed by the hand, based on visual and proprioceptive feedback.

### Recruitment of wrist movements and muscles

All three tasks required the same wrist movement. A typical trial required the subject to flex the wrist downward by 25° and to maintain constant this flexion while following the horizontal path indicated by the lower surface or the colored line. The horizontal path was 5 cm long. An increase of ulnar deviation from 0 to 10° was necessary to reach the right extremity of the horizontal trajectory. A final supplementary flexion terminated the trial, when the hand put the peg into the hole or moved downward at the end of the colored line.

### Experimental conditions and protocol

The experiment was conducted in two sessions, with eight subjects participating in the first and five participating in the second. Both sessions were identical, except for the muscle on which the H-reflex was elicited (see following text). Before performing the experimental blocks, subjects performed 35 practice trials in each condition to become familiar with the virtual environment, so that no learning effect was noted during the experiment. Each session consisted of nine blocks of trials. Between each block, the subject could rest his or her wrist. Each condition (SF, PF$_0$, PF$_f$) was tested during three blocks of trials: two blocks of 35 trials and one with 15 trials. The H-reflex was elicited during both 35-trial blocks, whereas the supplementary 15-trial block was dedicated to recordings in the absence of electrical stimulation. For each session, block order was randomized.

### Data acquisition

EMG. Two pairs of antagonistic muscles were recorded: flexor carpi radialis (FCR), extensor carpi radialis (ECR); flexor carpi ulnaris (FCU), extensor carpi ulnaris (ECU). The muscular activity was recorded with bipolar surface electrodes (Delsys Bagnoli 8). EMG signals were preamplified, band-pass filtered at 20–500 Hz, and sampled at 4,000 Hz. Temporal EMG patterns were quantified by computing the root-mean-square signal averaged over a sliding 50-ms time window. EMG collection encompassed the entire movement duration, but was then quantified only for the horizontal portion of the hand trajectory.

H-REFLEX. During the first session, the excitability of the motoneuron pool by afferent fibers (H-reflex) was tested in FCR with constant-current stimulation applied to the skin above the median nerve at the elbow (square pulse, 1-ms duration; DS7A, Digitimer, Hertfordshire, UK). The second session was dedicated to the study of the ECR H-reflex. The H-reflex could be evoked for ECR in only some individuals (five subjects) by stimulation of the radial nerve. We chose the stimulation location by monitoring on-line (with an oscilloscope; Tektronix TDS 210) the twitch responses in the target muscle as the stimulating electrode was moved over the skin. A supplementary clue used to find the best stimulus location was given by the sensations verbally reported by subjects when the intensity of stimulation was increased.

To elicit the H-reflex response during the experiment, constant-current electrical stimuli were applied via computer control of the stimulator at five different current levels. The selection of the stimulus intensities was carried out as follows: before the beginning of experimental blocks a complete recruitment curve was acquired for each muscle by applying a range of currents from subthreshold to that which evoked a maximal M-wave (M$_{max}$). Throughout the acquisition of the recruitment curve, subjects were asked to apply a force similar to the force they applied on the virtual surface during the experimental task. Five different intensities of stimulation on the ascending limb of the recruitment curve were chosen for the subsequent movement trials. The stability of the arm posture, which could also affect the reproducibility of the nerve stimulus, was ensured by the placement of the joystick and the trough constraining the arm posture.

Irrespective of the condition (SF, PF$_0$, PF$_f$), the H-reflex was elicited at one of three locations spaced evenly along the horizontal part of the trajectory. The current stimulus was triggered automatically at the selected location, based on position information provided in real time by the motion-tracking system (Coda Motion cx1, Charnwood Dynamics). The precise trigger time of the reflex was indicated by a synchronization signal from the electrical stimulator that was recorded in parallel with the EMG signals. For each of the three movement conditions, and for each muscle, 70 stimuli in all (5 intensities $\times$ 3 surface locations $\times$ 5 repetitions) were applied, each on a separate movement trial. The five intensities of stimulation and

the three horizontal locations were pseudorandomly distributed across trials within an experimental block.

TONIC EMG CALIBRATION. Before and after the experimental blocks, subjects performed a calibration task that consisted of exerting isometric forces against the joystick when it was locked at its center position. Eight directions (0, 45, 90, 135, 180, 225, 270, and 315°, where 0° points to the right) and four levels of force (4, 8, 12, and 16 N) were tested. For each trial, a reference force vector was displayed on the screen, showing the direction and amplitude of the force to be produced. Subjects were asked to reproduce the same force vector by pressing against the joystick. The exerted force was displayed in real time on the basis of the information provided by the force sensors of the joystick. When both vectors were stably superposed, EMG signals were acquired during 4 s. This test allowed us to identify the preferred direction for each muscle. The maximal signal obtained was used to normalize EMG traces of each muscle.

### Data acquisition and analysis

As described earlier, EMG and force data were analyzed only for the horizontal portion of the trajectory. EMG traces showed variations according to the position on the $x$-axis. Moreover, during the surface-following task, differences in the applied force could appear between the early and late phases of the movement. We therefore divided the horizontal portion of the trajectory into three regions—R1, R2, and R3—spanning 1 cm each and computed position, force, and EMG data within each of these regions, averaged across all trials for a given condition and a given subject.

EMG ACTIVITY DURING MOVEMENT. EMG recordings were full-wave rectified and averaged across all the trials of a given condition for each subject. We thus obtained the EMG patterns for the different types of tasks. The maximal EMG signal of each muscle obtained during the tonic EMG calibration was used to normalize EMG levels. EMG magnitudes are therefore reported in normalized units varying between 0 and 1.

H-REFLEXES. The background EMG activity was determined for each H-reflex trial. Prestimulus EMGs were rectified and averaged over a period of 25 ms to give a measure of muscle activation immediately before each reflex recording.

To compare H-reflexes under different conditions, the corresponding M-waves were considered as reliable indicators of the effective stimulus strength, i.e., under the assumption that for similar M-waves the same numbers of efferent and afferent fibers were excited. The recorded H-reflex was therefore compared across conditions for similar M-waves.

The five intensities of stimulation gave M-wave/H-wave (M–H) pairs corresponding to the ascending limb of the recruitment curve. An off-line analysis was performed with a custom-written Matlab program. Temporal windows were set to measure the peak-to-peak amplitude of the M- and H-waves. For each condition, M–H pairs were rank-ordered according to M-wave size. The least-mean-square linear regression line was fitted for each data set.

We calculated two representative values for the H-reflex for each condition, corresponding to two different stimulation intensities. We calculated the maximal H response ($H_{max}$) by averaging five maximal H-waves in each condition. The M-wave that evoked an H-wave equal to 50% of $H_{max}$ was then obtained in the control ($PF_0$) condition, a value that we denote as $M_{mid}$. The amplitude of the H-wave for the same stimulus intensity ($H_{mid}$) was obtained by inserting $M_{mid}$ into the regression equation for each of the other two conditions. We chose to compare H-wave amplitudes for two different stimulus intensities because facilatory and inhibitory effects are more visible on the ascending limb of the recruitment curve (Crone et al. 1990) since they mostly affect the motoneurons that are recruited last (Pierrot-Deseil-

ligny and Mazevet 2000). This method is robust regarding the small changes in M-wave that accompany wrist flexion.

### Statistical analysis

Averaged position, movement speed, force, and EMG signals for each muscle were analyzed with a $3 \times 3$ repeated-measures ANOVA [3 conditions ($PF_0$, $PF_f$, SF) $\times$ 3 regions (R1, R2, R3)]. A single-factor ANOVA assessed differences in the prestimulus activation and in the peak-to-peak amplitudes of the H responses ($H_{mid}$ and $H_{max}$) for FCR and ECR as a function of condition ($PF_0$, $PF_f$, SF). Tukey's test was used post hoc to identify the source of significant main effects. Statistical significance was set at $P \leq 0.05$ and descriptive statistics indicate the mean value $\pm$ SD. The SD is used in graphs of results to give an indication of the intersubject variability, whereas we rely on the ANOVA and post hoc tests to indicate when sample means differed significantly. $F$-values and degrees of freedom are reported in Table 1.

## RESULTS

All subjects reported the sensation of sliding along a rigid wall in the SF condition and a noticeable instability in the $PF_0$ and $PF_f$ conditions. They nevertheless successfully managed to perform each of the three movements.

### Tonic muscle activity

Figure 3 shows the activity of the four measured muscles as a function of force direction as measured in one subject during the isometric force production task (control task) performed prior to the experiment. Flexor activation generated downward force at the hand while extensor activation pushed upward. To obtain the muscle preferred direction we calculated the maximum correlation angle between the positive range of the cosine function and the EMG levels (Osu and Gomi 1999). The average preferred direction was $226 \pm 21°$ for FCR, $267 \pm 35°$ for FCU, $91 \pm 18°$ for ECR, and $63 \pm 21°$ for ECU, where 90 and 270° correspond to upward and downward forces, respectively. FCR and ECR act antagonistically when contributing to flexion/extension movements but they could contribute syner-

TABLE 1. *Summary of statistical results*

| | Region $F_{(2,14)}$ | Condition $F_{(2,14)}$ | Cross $F_{(4,28)}$ |
|---|---|---|---|
| Vertical position | 1.094 | 0.0433 | 0.802 |
| Horizontal velocity | 18.157*** | 10.366** | 0.0433 |
| Vertical force | 28.65*** | 36.863*** | 2.96* |
| FCR | 9.197** | 23.694*** | 1.396 |
| ECR | 3.96* | 5.72* | 2.503 |
| FCU | 0.307 | 10.352** | 0.435 |
| ECU | 2.185 | 5.425* | 0.258 |
| | | Condition $F_{(2,14)}$ | |
| FCR prestimulus activation | | 24.755*** | |
| FCR $H_{mid}$ | | 13.67*** | |
| FCR $H_{max}$ | | 8.58** | |
| | | Condition $F_{(2,8)}$ | |
| ECR prestimulus activation | | 2.163 | |
| ECR $H_{mid}$ | | 0.586 | |
| ECR $H_{max}$ | | 0.948 | |

Position, velocity, force, and EMG data were subjected to a two-way ANOVA (condition $\times$ region). Prestimulus activation and H reflex data were subjected to a single-factor ANOVA (condition). *$P < 0.05$; **$P < 0.01$; ***$P < 0.001$.
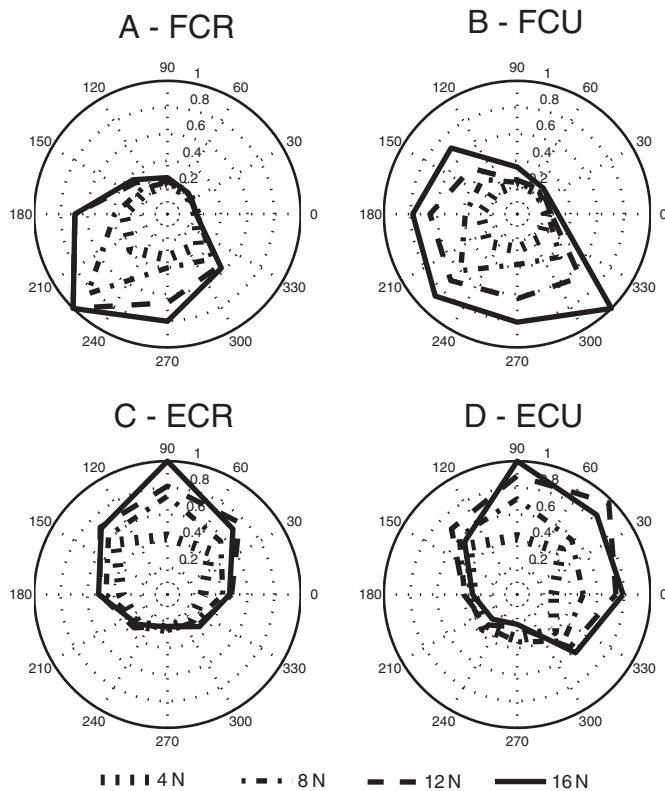
FIG. 3. Directional preferences of muscles' activities recorded during the calibration task. Subjects exerted isometric forces successively in each of 8 directions (0, 45, 90, 135, 180, 225, 270, 315°) at 4 levels of force (4, 8, 12, and 16 N). An orientation equal to 0 and 90° corresponded respectively to the rightward *x*-axis (horizontal movement) and upward *y*-axis (vertical movement) of the joystick and on the screen. Data from one subject: FCR (*A*), FCU (*B*), ECR (*C*), ECU (*D*).

gistically to radial deviation (abduction) at the wrist. In the primary experiment reported in the following text, the task required flexion and ulnar deviation of the wrist. Thus in the context of this experiment, FCR and ECR formed an antagonistic pair of opposing muscles. Conversely, although FCU and ECU also act antagonistically in wrist flexion and extension, they could act synergistically for ulnar deviations (adduction). These muscles could therefore contribute synergistically to the rightward displacement of the joystick. With respect to the primary focus of this experiment, however (i.e., the control of impedance perpendicular to the hand path and surface), the wrist flexors FCR and FCU were agonists and ECU and ECR were antagonists.

*Trajectory and force profiles*

Figure 4 illustrates the characteristics of the hand kinematics and dynamics as a function of the horizontal position of the hand and the results of the accompanying statistical comparisons. Figure 4*A* illustrates the similarity of the mean hand path in each of the three conditions. Irrespective of whether a bias force was imposed in free space, the hand trajectory was essentially the same (no main effects) as when the hand slid along the surface, whatever the region ($P = 0.362$) or the condition ($P = 0.958$). Due to the constraints placed on the forearm by the trough, a similar joystick trajectory means that the wrist performed the same movement across conditions.

Horizontal velocity varied as a function of horizontal position (Fig. 4*B*) such that the ANOVA signaled a main effect according to the region ($P < 0.001$). Peak velocity varied from $9.09 \pm 2.8$ cm·s$^{-1}$ in the PF$_0$ condition to $12.15 \pm 5.75$ cm·s$^{-1}$ in the SF condition and there was a significant main effect of condition in the ANOVA ($P = 0.002$). Average velocity when sliding along the surface (SF) was statistically greater than each of the other two conditions ($P < 0.01$).

Force profiles (Fig. 4*C*) reflect the constraints of the environment. The PF$_0$ condition was characterized by a near-zero vertical force ($0.48 \pm 0.33$ N), whereas the vertical forces were similar in the PF$_f$ ($5.61 \pm 0.85$ N) and SF ($4.95 \pm 1.8$ N) conditions. The observable differences in force across conditions were confirmed by a main effect in the ANOVA ($P < 0.001$). Post hoc analyses showed that the force level was significantly different in the PF$_0$ condition compared with SF or PF$_f$ ($P < 0.001$). However, the average force profiles exhibit only a slight gap between SF and PF$_f$ with no statistical difference ($P = 0.462$); i.e., the forces developed by subjects in free movement with a bias force (PF$_f$) and in the constrained environment (SF) were comparable. Note that there was a significant main effect of region on the vertical force ($P < 0.001$) and a significant cross-effect between region and condition ($P = 0.037$). Contact forces decreased as the hand moved from left to right in the SF condition ($P < 0.01$).

One might expect to find the vertical force to be strictly equal to zero for PF$_0$ since no physical constraint was programmed for this condition. On the contrary, we measured a small, constant downward force of the hand on the joystick ($<0.5$ N), which could be attributed to the geometry of the bearing mechanism. The distribution of mass on either side of the joystick's rotational center was not perfectly equal. The slightly greater weight of the backstage of the joystick created a small imbalance, which tended to bring the handle back to its central resting position when the handle was pushed downward. As was the case during the experiment, this imbalance resulted in a constant upward force of the joystick against the hand. Nevertheless, this small bias force was much weaker than either the bias force intentionally imposed by the system in PF$_f$ or the average downward force voluntarily exerted by the subject against the surface in the SF condition.

*FCR H-reflex*

Figure 5*A* plots H-wave amplitude as a function of M-wave amplitude for different stimulation intensities (five intensities of stimulation on the ascending limb), illustrating the partial recruitment curve across all conditions for one subject during one experimental session. There is significant variability in the H-wave amplitude for a given M-wave amplitude, but the regression analysis indicates how the H-reflex varies as a function of stimulus strength (as measured by the M-wave amplitude) and as a function of the movement conditions (PF$_0$, PF$_f$, SF). Figure 5*B* shows an example of the M- and H-waves averaged over the five maximal intensity levels for two conditions in a single subject.

As shown on Fig. 6*A*, the level of prestimulus activation in FCR differed across conditions ($P < 0.001$). In the PF$_f$ condition subjects exhibited a significantly greater FCR EMG level (normalized EMG = $0.25 \pm 0.1$) compared with PF$_0$ and SF ($P < 0.001$), whereas the level of FCR activation was
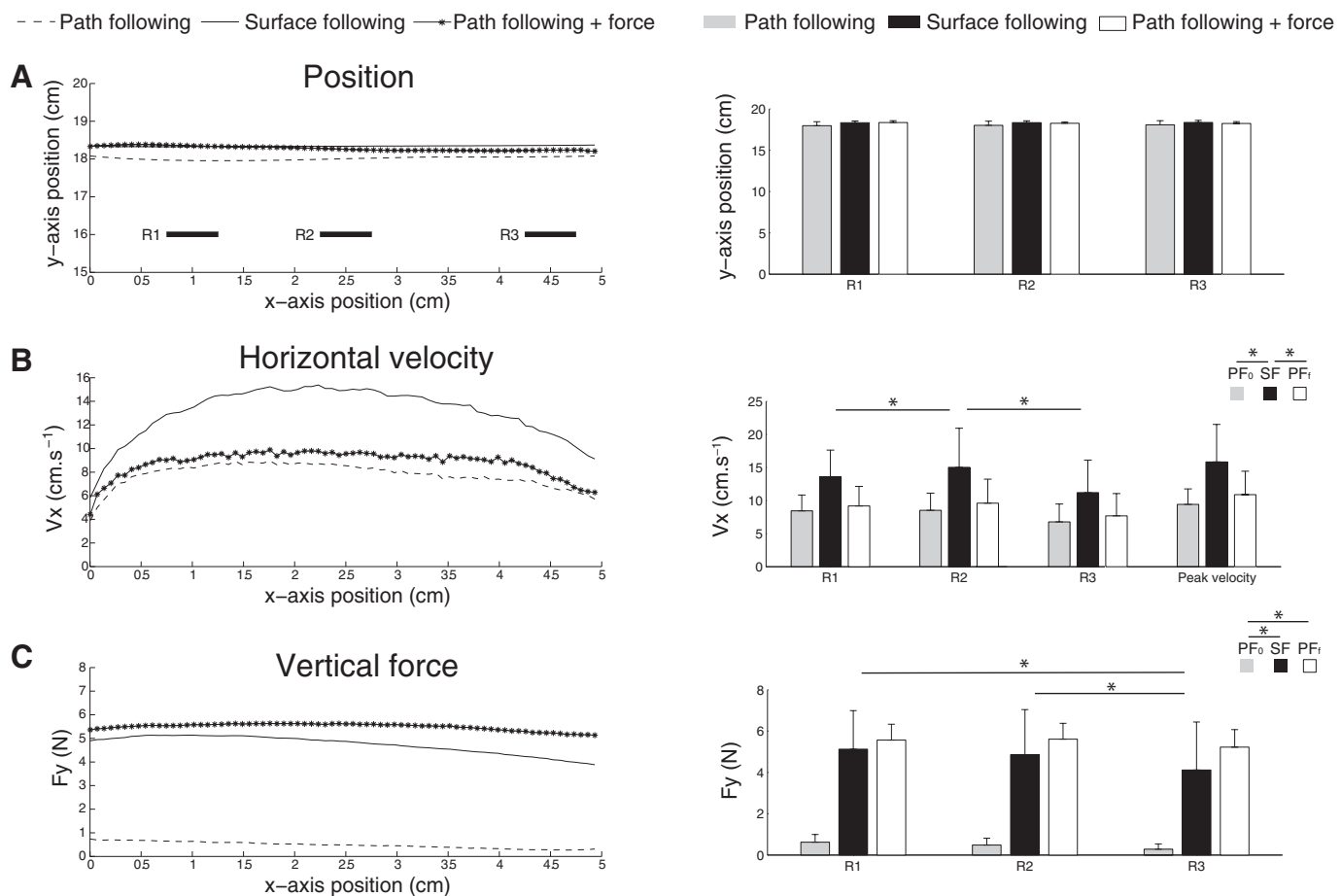
FIG. 4. Vertical position (*A*), horizontal velocity (*B*), and vertical force (*C*) profiles. Data are plotted vs. the horizontal position within the 5-cm span indicated in Fig. 2. Bars R1, R2, and R3 denote the different regions used to compute and compare data for the statistical analysis. Data are shown averaged across all subjects. Bar graphs show averaged data across all subjects for each region: R1, R2, and R3. The average value of the peak velocity is also displayed. The *y*-position is similar along the trajectory irrespective of condition, whereas the velocity of the movement depends on the condition and region. There was no significant difference in the force level between SF and $PF_f$ conditions. Values are means $\pm$ SD for 8 subjects (*$P < 0.05$).

similar in SF ($0.15 \pm 0.08$) compared with $PF_0$ ($0.13 \pm 0.07$; $P = 0.436$). The larger flexor activation noted for $PF_f$ was due to the need to counteract the effects of the force field, although this imposed force constraint could not by itself explain the greater activation of FCR. The force applied against the surface in the SF condition was similar to the force applied in $PF_f$, but with a lower level of flexor activation. This implies a lower level of coactivation in the antagonist muscles when the force was exerted against the rigid surface (see following text).

A task-dependent augmentation of the H-reflex was found on every subject such that the FCR H-reflex was systematically larger during surface following (SF) and when working against the added force load ($PF_f$), compared with the task of following an unconstrained trajectory ($PF_0$). In Fig. 6*B*, the average amplitude of the H-reflex in each of the three conditions is plotted, for which we found a main effect of condition on $H_{mid}$ ($P < 0.001$) and $H_{max}$ ($P < 0.01$). Overall, H-reflexes taken from the ascending limb of the M–H curve ($H_{mid}$) were significantly larger for SF ($0.42 \pm 0.32$) and $PF_f$ ($0.41 \pm 0.3$) compared with $PF_0$ ($0.22 \pm 0.2$; $P < 0.01$). Maximum H-reflex amplitude ($H_{max}$) showed the same pattern (PF: $0.31 \pm 0.26$; SF: $0.57 \pm 0.35$; $PF_f$: $0.62 \pm 0.35$; $P < 0.01$). The greater H-reflex amplitude in $PF_f$ compared with $PF_0$ could be the result of the more pronounced prestimulus activation in the

former condition because it is known that the H-reflex depends on which motoneurons are recruited in the target motoneuron pool (Matthews 1986b). In contrast to this, however, FCR prestimulus activation was similar in $PF_0$ and SF ($P = 0.436$): the background activation of the motoneuron pool could therefore not explain the difference observed in H-reflex amplitude. This is evidence for a task-specific modulation of the FCR H-reflex as a function of the force exerted by the wrist, independent of the muscle activity required to produce that force.

### ECR H-reflex

Having shown that FCR H-reflexes were task dependent during a movement requiring wrist flexion, we decided to investigate the spinal excitability of ECR as well, an FCR antagonist. Despite the difficulty of recording H-reflex on ECR during wrist flexion, we succeeded in doing so on five subjects. The relatively low level of global muscular activity (the force generated never exceeded 8 N) facilitated this task. As shown in Fig. 6*C*, the levels of prestimulus activation of ECR did not differ significantly across conditions (no main effect for condition, $P = 0.18$) even if one can note a trend to a lower activity in SF ($0.22 \pm 0.03$) compared with $PF_0$ ($0.28 \pm 0.07$)

○ Path following  × Surface following  △ Path following + force

**A**

**B**

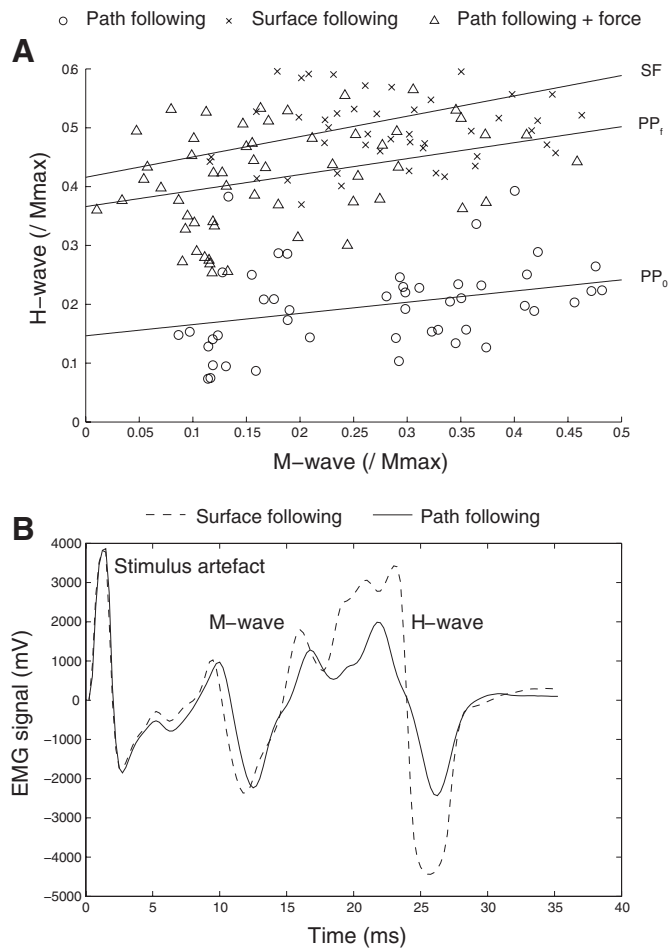- - - Surface following  ——— Path following

FIG. 5. Examples of H-reflex data for one subject. *A*: M-wave/H-wave (M–H) recruitment curves across all 3 conditions. *B*: trace obtained by averaging the electromyographic (EMG) signal corresponding to the 5 maximal H-waves of the M–H recruitment curve for $PF_0$ and SF.

to reveal the direction of the difference. The significant effect of region on FCR and ECR indicates that the balance between flexor and extensor activities was not exactly the same between the beginning and the end of the movement, although the lack of statistical significance for the other muscles leaves in doubt whether the pattern of activation was symmetric between agonist and antagonist muscles.

Significant main effects of condition on EMG levels were seen in all muscles (FCR: $P < 0.001$; ECR: $P = 0.015$; FCU: $P = 0.002$; ECU: $P = 0.018$). Post hoc tests revealed the most striking element: the activity of muscles was systematically larger in $PF_f$ compared with SF ($P < 0.001$ for flexors; $P < 0.02$ for extensors), even though the net forces produced on the environment in both these conditions were equivalent. The fact that both flexor and extensor activity increased indicates a greater level of coactivation in the $PF_f$ condition compared with SF. A comparison of EMG patterns between $PF_0$ and SF complements these observations. At the center horizontal location, activity of flexors was quite similar in $PF_0$ and SF (FCR: $0.18 \pm 0.09$ vs. $0.19 \pm 0.1$; FCU: $0.41 \pm 0.2$ vs. $0.44 \pm 0.16$), even though there was essentially no net downward force required in the $PF_0$ condition. Flexor activation in free space was similar to that required to produce a 5-N force against a rigid surface. Extensor traces showed a larger activity in $PF_0$ than in SF (ECR: $0.28 \pm 0.11$ vs. $0.19 \pm 0.1$; ECU: $0.36 \pm 0.16$ vs. $0.3 \pm 0.15$), although no statistical difference was found between these conditions in post hoc analysis. Note that a less-conservative Newman–Keuls post hoc test does detect a significant difference between these two cases for ECR.

The absence of any environmental constraint resisting the increased flexor contraction in $PF_0$ suggests that greater activation of extensors in the unconstrained case must be present, even if the evidence is statistically less reliable. To further test whether EMG signals from the two extensors in these two conditions indeed indicated supplementary activation of these muscles above resting levels, we compared ECR and ECU EMG levels in $PF_0$ and SF with the minimal EMG levels observed in the measurements of tonic muscle activity from the isometric control task. In this latter situation, in which the joystick was rigidly maintained in the center position, the stability of the hand and joystick position was absolute and one would expect a minimum level of cocontraction when exerting a significant force in a given direction. Thus for downward forces exerted by the wrist, extensors would be essentially at rest. In a supplementary ANOVA analysis we found that EMG activity was higher in ECR for $PF_0$ ($P < 0.02$), but not SF, as compared with the minimal value in the isometric condition. This indicates that there was indeed a certain level of coactivation between FCR and ECR in the $PF_0$ condition. Although no statistical difference in activation was observed for ECU between $PF_0$ and SF, both conditions resulted in higher ECU activation compared with the minimal value in the isometric control. Some level of ECU activation appears to occur in all cases, perhaps because this muscle contributes to the ulnar deviation of the wrist in addition to its role as a wrist extensor.

and $PF_f$ ($0.26 \pm 0.07$). The amplitude of ECR H-reflex (Fig. 6*D*) was equivalent whatever the condition ($P = 0.37$). The modulation of the motoneurons' excitability with output force in this task appears to be restricted to the FCR pool.

*EMG patterns*

For these experiments, subjects were not requested to maintain a specified EMG level, so the observed EMG patterns were the consequence of the task requirements and the strategy put in place by the CNS. We plotted the EMG patterns from four muscles according to the position on the *x*-axis in Fig. 7. The data used for the statistical analysis are shown in Fig. 7. A main effect for region was found only in the flexor FCR ($P < 0.01$), one of the main agonist muscles used to apply a force against the surface. Activity was higher for R1 (i.e., at the time of horizontal movement initiation) compared with the other two regions ($P < 0.02$). The other recorded flexor exhibited the same trend with an initial activity more pronounced than the activity recorded at the end of the horizontal trajectory, but this trend was not statistically significant. Extensors followed the opposite tendency, showing activity that increased along the trajectory. These differences reached statistical significance only for ECR, as revealed by a main effect in the ANOVA ($P < 0.05$), but post hoc tests failed

DISCUSSION

We assessed the tonic muscular activation and reflex excitability during different types of movements with the wrist. Compared with a path-following movement without force

A   FCR pre-stimulus activation
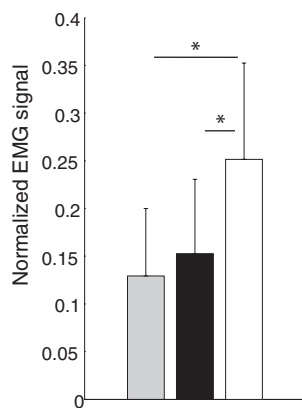
ECR pre-stimulus activation
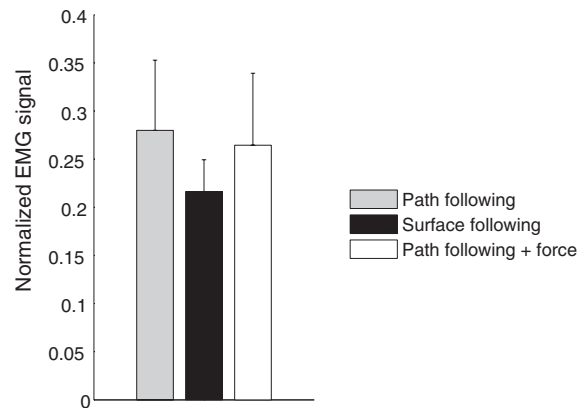


B   FCR H-reflex amplitude
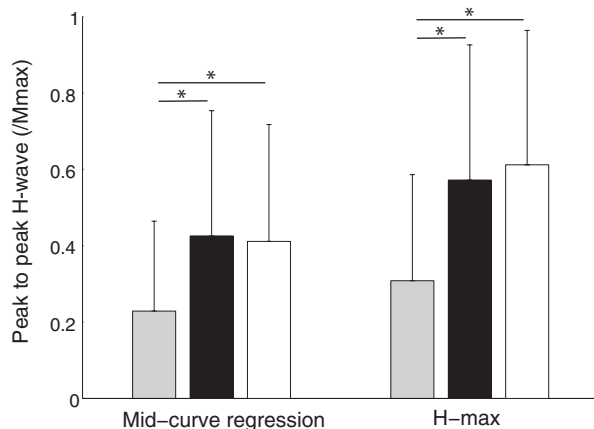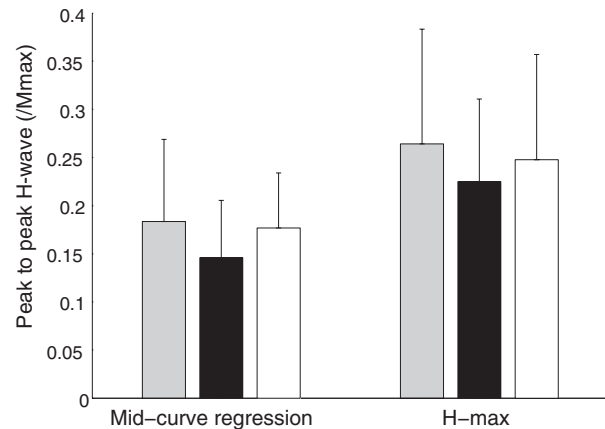
ECR H-reflex amplitude



FIG. 6. Prestimulus activation (*A*) and H-reflex (*B*) for flexor carpi radialis (FCR) and extensor carpi radialis (ECR). Data shown are averaged across all 8 subjects. A significant increase of FCR activity is noted in the $PF_f$ condition. No significant differences are observed between the 3 experimental conditions for ECR. The FCR H-reflex amplitude is increased in SF and $PF_f$ conditions compared with $PF_0$ condition, whereas ECR H-reflex amplitude is constant whatever the condition. Values are means ± SD for 8 subjects (*$P < 0.05$).

($PF_0$), the presence of an external force in free space ($PF_f$) resulted in more pronounced coactivation of antagonistic muscles. With regard to the surface-following task (SF), lower activation of extensors (i.e., minimal coactivation) was observed compared with free movements, particularly when we compared movements generating the same net force against the environment. Because $PF_f$ differed from SF not in the external force to be produced, but in the stability requirements, we can conclude that coactivation is used to counteract the destabilizing effect of the extra force in free space by making the joint stiffer. In the case of the interaction against the surface, the solid support obviated the need for the stabilizing effect of coactivation, even as the net force increased.

These observations show that the CNS uses coactivation of antagonists to deal with unexpected external forces when performing unconstrained movements in free space. On the other hand, H-reflex amplitude in the agonist muscle (FCR) was greater for constrained (SF) than for unconstrained ($PF_0$) movements. In contrast to our hypotheses, the CNS does not appear to reduce the gain of the stretch reflex so as to increase compliance with an external constraint. Instead, the reflex gain, as indicated by the strength of the H-reflex, appears to be coupled to the net force applied by the hand to the environment. The other original finding is the dissociation between H-reflex amplitude and the muscular activity. The condition in free space with external force ($PF_f$) evoked higher H-reflex amplitude in FCR than one might expect as a consequence of the increased flexor activity.

These results provide new information about how the human motor system handles dynamic interactions with the environment. In the following we discuss methodological issues linked to the H-reflex technique so as to eliminate these factors as the source of these novel observations. We then discuss these results in terms of the dynamical requirements on the motor control system for these tasks and in terms of the underlying physiological mechanisms.

*Methodological issues*

The H-reflex technique is widely used, but seldom in the case of truly natural movements. What are the potential pitfalls of such studies? If one assumes that both presynaptic inhibition and postsynaptic inhibition remain constant, the primary factor affecting the amplitude of the H-reflex is the afferent volley
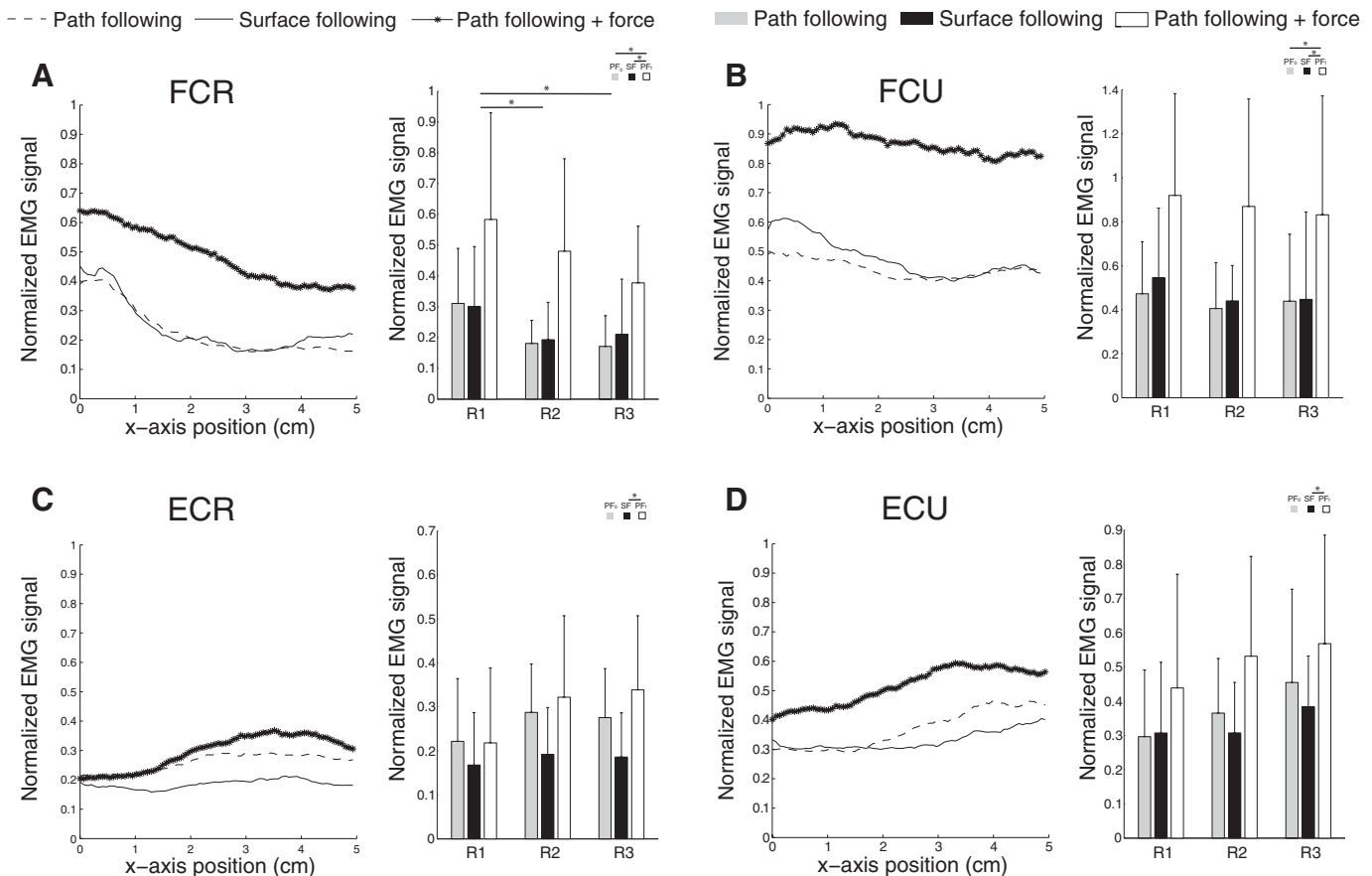
- - - Path following ——— Surface following ——*— Path following + force

▨ Path following  ■ Surface following  ▢ Path following + force



FIG. 7. EMG activity of FCR (*A*), flexor carpi ulnaris (FCU, *B*), ECR (*C*), and extensor carpi ulnaris (ECU, *D*) plotted vs. the horizontal position along the trajectory (*left*) and averaged for each region R1, R2, and R3 (*right*), for all 3 conditions (mean values for all 8 subjects). Bar graphs show averaged data across all subjects for each region: R1, R2, and R3. As shown by the plots of extensor activation, the level of coactivation was largest in PF$_f$. Values are means $\pm$ SD for 8 subjects (*$P < 0.05$).

driven by Ia afferents acting on motor neurons (Crone et al. 1990). Consequently, it is crucial to check that the synaptic input is constant during an experiment. The major problem that arises with surface nerve stimulation in these studies is the potential shift of the electrode location relative to the nerve. This phenomenon leads to variations of Ia afferent activation that is independent from any potential modulation of the reflex gain. We minimized the movement of the electrode over the nerve thanks to the trough structure that braced the forearm. Furthermore, trial-to-trial variations of M-wave were taken into account since the regression was done on M–H pairs. Finally, after each block of 35 trials, we measured the maximal M-wave and used this value to normalize data (Zehr 2002).

Another factor affecting the amplitude of the reflex is the interstimulus interval (ISI). It has been shown that the amplitude of H-reflex diminishes when stimuli are closely spaced in time. On the upper limb, the recovery between two stimulations is achieved in <1 s (Rossi-Durand et al. 1999). In our experiment, the ISI could fluctuate according to the time necessary for subjects to initiate the task or follow the indicated path. Considering the time necessary to initialize the joystick for each trial, ≥10 s elapsed between two successive stimulations. This should be long enough to avoid any attenuation effects between two stimuli closely spaced in time.

Movement velocity may also have an effect on H-reflex amplitude. When actively or passively pedaling, increasing the velocity of the movement inhibits the soleus H-reflex (McIlroy et al. 1992). To our knowledge, similar data are not available for the upper limb, although Carroll et al. (2006) showed an increase of corticospinal excitability (H-reflex and motor evoked potentials) during cycling movements of the arm compared with tonic contractions. We cannot exclude the intervention of a hypothetical central pattern generator in such rhythmic movements: the modulation observed might therefore be specific to locomotor schemes. Nevertheless, according to these data, we would expect a decrease of the H-reflex amplitude in the SF condition because these movements were the fastest. Even if the difference in speed across conditions was great enough to diminish H-reflex amplitude for the higher velocities, it seems that this factor had a weak contribution compared with others that increased the H-reflex as the net force increased.

### Implications for motor control

Whether the interaction with the environment is a force field or a rigid surface, subjects appear to modulate limb impedance according to the nature of the mechanical interaction. Chib et al. (2006), by varying the stiffness of an obstacle in the environment, classified the responses in two categories: subjects increased their resistance to low stiffness obstacles, whereas they tended to reduce their force output and conform

to contact with high stiffness objects. The observations recorded here about the level of contraction are in accordance with these adaptive behaviors. Through coactivation the CNS stabilizes the hand and enforces the planned trajectory in free space. On contact with a rigid object, however, subjects relaxed their muscles to comply with the constraint.

Coactivation is the most robust strategy to counteract perturbations, whatever their frequency (Humphrey and Reed 1983). The functional significance of coactivation of antagonistic muscles is an increase of joint stiffness (Feldman 1980; Joyce et al. 1969; Nichols and Houk 1976). It is often cited as a way to escape destabilizing dynamics (Milner 2002; Osu and Gomi 1999). Wrist muscles were also much more coactivated when they resisted an unstable load compared with a constant or elastic load (De Serres and Milner 1991). The force imposed in $PF_f$ was constant along the movement, contrary to many studies where strong unpredictable instabilities were imposed. Nevertheless, compared with surface following, for which the stability of the hand is ensured by the rigidity of the surface, the $PF_0$ and $PF_f$ conditions were more unstable. As evidenced by the higher overall muscle activation in $PF_0$ and $PF_f$ compared with SF, the CNS appears to maintain stability in free space through increased coactivation. This may, in fact, be the simple reflection of stability constraints. The use of neural feedback to react to external forces, rather than coactivation, would threaten stability in free space. Due to the presence of delay in neural transmission, feedback loop gains cannot theoretically exceed 1 (Bennett et al. 1994) and feedback must be limited to low frequency.

Doemges and Rack (1992), in a study of the long-latency stretch reflex, described an increase of reflex gain in a "maintain flexed position task" (analogous to staying on the visual path in $PF_0$ and $PF_f$) compared with a "maintain flexing force case" (analogous to the task of controlling forces against the rigid constraint in SF). The reflex amplitude in this earlier study did not appear to be coupled to the force exerted but rather to the intended interaction with the environment. Their results seem to conform to the hypothesis we initially formulated—i.e., that reflex gains would be low for a constrained interaction (maintain force) and high for a movement or posture in free space (maintain position), and in opposition to the augmentation of the H-reflex we noted in SF (also a maintain-force task). Similarly, Perreault et al. (2008) reported a decrease in stretch reflex sensitivity during multijoint interactions with a compliant environment. One explanation may be in the reflex responses that were examined. To the extent that the H-reflex is a manifestation of short-latency reflex response, the response may contrast with the long-latency responses measured in these other studies. Indeed, in the report by Doemges and Rack (1992), the earliest reflex responses appear to be similar in the maintain-position versus the maintain-force tasks (Fig. 4), even if the long-latency responses were significantly different. An alternative explanation may be found in the differences between the tasks performed in each study. In both cited experiments, subjects had to maintain a constant force despite movements of the rigid constraint. The stretch reflex, by resisting the imposed movement, could be detrimental to the maintenance of a constant force. On the contrary, in our study, subjects determined themselves the force to exert against the surface and the surface did not move. In the latter case the system may profit

from the automatic reinforcement of the agonist activity by the spinal loop to ensure the contact with a rigid object, in much the same way that a robot can avoid chatter through a positive force feedback loop. Maintaining a stable interaction was the primary goal of the motor activity in our task and the magnitude of the force exerted was not explicitly regulated. Consequently, the demands of the task reported by Doemges and colleagues and Perreault and colleagues appear to be different.

Is there a strict coupling between muscle activation and H-reflex amplitude, or can these mechanisms act independently? Akazawa et al. (1983) reported a stretch reflex increase in flexor pollicis longus when subjects maintained constant the position of their thumb against variable and constant loads, but the change in reflex reported in these situations could be attributed to the increase of tonic muscle activation. More surprisingly, we found a similar H-reflex increase in FCR during the surface-following task (SF), even though the level of flexor activation remained low. The amplitude of the H-reflex clearly depended on factors other than the prestimulus EMG activity. Based on the observations reported here, it may be that the H-reflex amplitude depends more on the force exerted on the environment, independent of the muscle activation needed to produce that force, since both conditions requiring force production led to an increased H-reflex. Task-specific changes to the reflex amplitude/muscle activation relationship could also explain these observations.

The increase of reflex sensitivity for constrained motion goes against the principle of impedance modulation evoked in the INTRODUCTION. One would expect reflex gains to diminish for constrained motion so as to augment the compliance of the limb. Furthermore, we observed H-reflex modulation only in the agonist, force-producing muscle. From the perspective of impedance modulation per se, one would expect gains in both sets of muscles to be modulated in parallel. Finally, gains increased even when stability was less of a factor (i.e., in the case of constrained motion). These observations argue for alternative explanations for the purpose of the stretch reflex. For instance, reflexes can complement intrinsic biomechanical properties. They can compensate for the phenomenon of muscle yielding and may serve to linearize the force–stiffness relationship (Nichols and Houk 1976). In this light, coactivation and reflex mechanisms would work together to impart desirable impedance properties to the limb.

### Spinal networks and modulation of H-reflex

Although little is known about the modulation of reflex gains in the upper limp, we can compare our surface- and path-following tasks with the modulation of the H-reflex in the lower limb: in both cases, the CNS has to deal with a rigid and a free environment. Capaday and Stein (1986) recorded a larger reflex during standing than that during walking. Furthermore, H-reflex gains vary according to the phase of the locomotor cycle; H-reflex in soleus is high during the stance phase and low during the swing phase. Thus H-reflex in the leg increases when producing force against the environment (i.e., supporting the weight of the body) in the same way that H-reflex in the wrist increased in our experiments when exerting a force against the environment with the hand.

The spinal pathways related to the wrist differ from those of the lower limb in some aspects, such as the presence of

interneurons governing nonreciprocal inhibition. During wrist flexion, the corticospinal tract excites both FCR motoneurons and group I interneurones that inhibit ECR (Day et al. 1983, 1984; Wargon et al. 2006). This organization would tend to reduce the stretch reflex in ECR while at the same time reducing FCR inhibition by ECR Ia afferents. The latter effect would in turn facilitate the H-reflex in FCR. These mechanisms, which serve to reinforce the central command over peripheral feedback, could explain why we saw H-reflex modulation only in FCR (the primary agonist) in our experiment.

In upper and lower limbs, afferent information entering the spinal cord can be modified before reaching the target motoneurons. Corticospinal projections converge on common spinal interneurons with peripheral afferents (Iles and Pisini 1992). This presynaptic inhibition has a crucial effect on the H-reflex gain since it particularly affects Ia terminals (Rudomin 1990). Indeed, by evoking heteronymous facilitation, Faist et al. (1996) were able to attribute H-reflex modulation in locomotion to presynaptic inhibition. The way in which presynaptic inhibition is modulated, however, is also specific to the upper body. Transcranial magnetic stimulation increases presynaptic inhibition of Ia afferents in the arm by facilitating presynaptic inhibition on Ia terminals (Meunier and Pierrot-Deseilligny 1998), whereas it reduces the influence of Ia terminals on lower-limb motoneurons (Hultborn et al. 1987). Despite these specificities of upper- and lower-limb circuitry, however, corticospinal pathways can modulate reflex gains in at least two ways: by modulating activity in type I interneurons and by presynaptic inhibition of afferent information imping-ing on the motoneuron.

The efficacy of the monosynaptic Ia stretch reflex at the wrist can also be tuned by peripheral factors. Cutaneous afferences tonically inhibit the Ia presynaptic inhibitory pathways (Aimonetti et al. 2000). This inhibition of inhibition would have the net effect of increasing the reflex gain when exerting forces through contact with the environment. Although speculative at this point, such a mechanism could explain why H-reflex increased in both $PF_f$ and SF, regardless of the muscular activity used to generate the force applied by the hand.

### Conclusion

By proposing two types of tasks, constrained motion along a rigid surface and free movements following a specified path, we have examined the ability of the CNS to tune its mechanical interactions with the environment. The measurements of muscular activities reported here bring new insights into the physiological processes that underlie the adaptation of the impedance. Impedance seems to increase notably in free space compared with constrained motion through the use of coactivation. On the other hand, spinal loop gains can be adjusted to better regulate the forces exerted by the hand on the environment, particularly when interacting with a rigid object. These observations are supplementary arguments supporting the hypothesis of movement programming in terms of impedance.

REFERENCES

**Aimonetti JM, Vedel JP, Schmied A, Pagni S.** Mechanical cutaneous stimulation alters Ia presynaptic inhibition in human wrist extensor muscles: a single motor unit study. *J Physiol* 522: 137–145, 2000.

**Akazawa K, Milner TE, Stein RB.** Modulation of reflex EMG and stiffness in response to stretch of human finger muscle. *J Neurophysiol* 49: 16–27, 1983.

**Bennett DJ, Gorassini M, Prochazka A.** Catching a ball: contributions of intrinsic muscle stiffness, reflexes, and higher order responses. *Can J Physiol Pharmacol* 72: 525–534, 1994.

**Burdet E, Osu R, Franklin DW, Milner TE, Kawato M.** The central nervous system stabilizes unstable dynamics by learning optimal impedance. *Nature* 414: 446–449, 2001.

**Capaday C, Stein RB.** Amplitude modulation of the soleus H-reflex in the human during walking and standing. *J Neurosci* 6: 1308–1313, 1986.

**Carroll TJ, Baldwin ER, Collins DF, Zehr EP.** Corticospinal excitability is lower during rhythmic arm movement than during tonic contraction. *J Neurophysiol* 95: 914–921, 2006.

**Chib VS, Patton JL, Lynch KM, Mussa-Ivaldi FA.** Haptic identification of surfaces as fields of force. *J Neurophysiol* 95: 1068–1077, 2006.

**Crone C, Hultborn H, Mazières L, Morin C, Nielsen J, Pierrot-Deseilligny E.** Sensitivity of monosynaptic test reflexes to facilitation and inhibition as a function of the test reflex size: a study in man and the cat. *Exp Brain Res* 81: 35–45, 1990.

**Day BL, Marsden CD, Obeso JA, Rothwell JC.** Reciprocal inhibition between the muscles of the human forearm. *J Physiol* 349: 519–534, 1984.

**Day BL, Rothwell JC, Marsden CD.** Transmission in the spinal reciprocal Ia inhibitory pathway preceding willed movements of the human wrist. *Neurosci Lett* 37: 245–250, 1983.

**De Serres SJ, Milner TE.** Wrist muscle activation patterns and stiffness associated with stable and unstable mechanical loads. *Exp Brain Res* 86: 451–458, 1991.

**Doemges F, Rack PM.** Task-dependent changes in the response of human wrist joints to mechanical disturbance. *J Physiol* 447: 575–585, 1992.

**Evarts EV, Tanji J.** Gating of motor cortex reflexes by prior instruction. *Brain Res* 71: 479–494, 1974.

**Faist M, Dietz V, Pierrot-Deseilligny E.** Modulation, probably presynaptic in origin, of monosynaptic Ia excitation during human gait. *Exp Brain Res* 109: 441–449, 1996.

**Feldman AG.** Superposition of motor programs—I. Rhythmic forearm movements in man. *Neuroscience* 5: 81–90, 1980.

**Franklin DW, Burdet E, Osu R, Kawato M, Milner TE.** Functional significance of stiffness in adaptation of multijoint arm movements to stable and unstable dynamics. *Exp Brain Res* 151: 145–157, 2003.

**Franklin DW, So U, Kawato M, Milner TE.** Impedance control balances stability with metabolically costly muscle activation. *J Neurophysiol* 92: 3097–3105, 2004.

**Hammond PH.** The influence of prior instruction to the subject on an apparently involuntary neuro-muscular response. *J Physiol* 132: 17–18, 1956.

**Hogan N.** Adaptive control of mechanical impedance by coactivation of antagonist muscles. *IEEE Trans Auto Control* 29: 681–690, 1984.

**Hogan N.** Mechanical impedance of single- and multi-articular systems. In: *Multiple Muscle Systems: Biomechanics and Movement Organization*, edited by Winters JM, Woo SL-Y. New York: Springer-Verlag, 1990, p. 149–164.

**Houk JC, Rymer WZ.** Neural control of muscle length and tension. In: *Handbook of Physiology. The Nervous System. Motor Control.* Bethesda, MD: Am. Physiol. Soc., 1981, sect. 1, vol. II, pt. 1, p. 257–323.

**Hultborn H, Meunier S, Pierrot-Deseilligny E, Shindo M.** Changes in presynaptic inhibition of Ia fibres at the onset of voluntary contraction in man. *J Physiol* 389: 757–772, 1987.

**Humphrey DR, Reed DJ.** Separate cortical systems for control of joint movement and joint stiffness: reciprocal activation and coactivation of antagonist muscles. In: *Motor Control Mechanisms in Health and Disease*, edited by Desmedt JE. New York: Raven Press, 1983, p. 347–372.

**Iles JF, Pisini JV.** Cortical modulation of transmission in spinal reflex pathways of man. *J Physiol* 455: 425–446, 1992.

**Joyce GC, Rack PM, Westbury DR.** The mechanical properties of cat soleus muscle during controlled lengthening and shortening movements. *J Physiol* 204: 461–474, 1969.

**Lacquaniti F, Licata F, Soechting JF.** The mechanical behavior of the human forearm in response to transient perturbations. *Biol Cybern* 44: 35–46, 1982.

**Matthews PB.** What are the afferents of origin of the human stretch reflex, and is it a purely spinal reaction? *Prog Brain Res* 64: 55–66, 1986a.

**Matthews PB.** Observations on the automatic compensation of reflex gain on varying the pre-existing level of motor discharge in man. *J Physiol* 374: 73–90, 1986b.

**McIlroy WE, Collins DF, Brooke JD.** Movement features and H-reflex modulation. II. Passive rotation, movement velocity and single leg movement. *Brain Res* 582: 85–93, 1992.

**McIntyre J, Gurfinkel EV, Lipshits MI, Droulez J, Gurfinkel VS.** Measurements of human force control during a constrained arm motion using a force-actuated joystick. *J Neurophysiol* 73: 1201–1222, 1995.

**Meunier S, Pierrot-Deseilligny E.** Cortical control of presynaptic inhibition of Ia afferents in humans. *Exp Brain Res* 119: 415–426, 1998.

**Milner TE.** Adaptation to destabilizing dynamics by means of muscle cocontraction. *Exp Brain Res* 143: 406–416, 2002.

**Nichols TR, Houk JC.** Improvement in linearity and regulation of stiffness that results from actions of stretch reflex. *J Neurophysiol* 39: 119–142, 1976.

**Osu R, Gomi H.** Multijoint muscle regulation mechanisms examined by measured human arm stiffness and EMG signals. *J Neurophysiol* 81: 1458–1468, 1999.

**Perreault EJ, Chen K, Trumbower RD, Lewis GN.** Interactions with compliant loads alter stretch reflex gains but not intermuscular coordination. *J Neurophysiol* 99: 2101–2113, 2008.

**Pierrot-Deseilligny E, Mazevet D.** The monosynaptic reflex: a tool to investigate motor control in humans. Interest and limits. *Neurophysiol Clin* 30: 67–80, 2000.

**Rossi-Durand C, Jones KE, Adams S, Bawa P.** Comparison of the depression of H-reflexes following previous activation in upper and lower limb muscles in human subjects. *Exp Brain Res* 126: 117–127, 1999.

**Rudomin P.** Presynaptic inhibition of muscle spindle and tendon organ afferents in the mammalian spinal cord. *Trends Neurosci* 13: 499–505, 1990.

**Selen LP, Beek PJ, van Dieen JH.** Impedance is modulated to meet accuracy demands during goal-directed arm movements. *Exp Brain Res* 172: 129–138, 2006.

**Smith AM.** The coactivation of antagonist muscles. *Can J Physiol Pharmacol* 59: 733–747, 1981.

**Tanji J, Evarts EV.** Anticipatory activity of motor cortex neurons in relation to direction of an intended movement. *J Neurophysiol* 39: 1062–1068, 1976.

**Wargon I, Lamy JC, Baret M, Ghanim Z, Aymard C, Penicaud A, Katz R.** The disynaptic group I inhibition between wrist flexor and extensor muscles revisited in humans. *Exp Brain Res* 168: 203–217, 2006.

**Zehr PE.** Considerations for use of the Hoffmann reflex in exercise studies. *Eur J Appl Physiol* 86: 455–468, 2002.